Journal of Applied Geophysics 133 (2016) 16–24

Contents lists available at ScienceDirect

Journal of Applied Geophysics

journal homepage: www.elsevier.com/locate/jappgeo

A non-linear induced polarization effect on transient electromagnetic soundings

Valeriya Yu. Hallbauer-Zadorozhnaya [a], Giovanni Santarato [b,*], Nasser Abu Zeid [b], Samuel Bignardi [b]

[a] Consultant Geophysicist, P.O. Box 1153, Silverton, Pretoria 0127, South Africa
[b] University of Ferrara, Via Saragat 1, I-44122 Ferrara, Italy

ARTICLE INFO

Article history:
Received 10 July 2015
Received in revised form 26 May 2016
Accepted 14 July 2016
Available online 16 July 2016

Keywords:
Induced polarization
TEM sounding
Non-linear effects
Membrane polarization

ABSTRACT

In a TEM survey conducted for characterizing the subsurface for geothermal purposes, a strong induced polarization effect was recorded in all collected data. Surprisingly, anomalous decay curves were obtained in part of the sites, whose shape depended on the repetition frequency of the exciting square waveform, i.e. on current pulse length.

The Cole–Cole model, besides being not directly related to physical parameters of rocks, was found inappropriate to model the observed distortion, due to induced polarization, because this model is linear, i.e. it cannot fit any dependence on current pulse. This phenomenon was investigated and explained as due to the presence of membrane polarization linked to constrictivity of (fresh) water-saturated pores. An algorithm for mathematical modeling of TEM data was then developed to fit this behavior.

The case history is then discussed: 1D inversion, which accommodates non-linear effects, produced models that agree quite satisfactorily with resistivity and chargeability models obtained by an electrical resistivity tomography carried out for comparison.

1. Introduction

In 2012, two authors (G. Santarato and N. Abu-Zeid) and Dr. M. Goldman (the Geophysical Institute of Israel, personal communication to V. Hallbauer-Zadorozhnaya) simultaneously recorded a non-linear behavior of Time domain Electro-Magnetic (TEM) signals collected at different repeat frequencies. The relaxation curves were affected by the typical induced polarization (IP) effect (Bhattacharyya, 1964), but their shape depended on current pulse length. To our knowledge, neither published data have reported similar behavior nor discussed this specific anomalous behavior, so that it can be considered as a "new" phenomenon, to be related to non-linearity of the IP effects. Our aim is to find out what type or types of polarization occur in the rocks that affect the induction processes occurring in the polarizable layers due to instantaneous current switch-off of in the transmitter loop, that produce such non-linear behavior.

It is well known that the IP phenomenon is due to at least four mechanisms, i.e. the so-called electrode polarization, electro-osmosis polarization, Maxwell–Wagner effect, and membrane polarization. The latter occurs due to presence of disseminated/dispersed clay minerals in rock pores and/or due to their constrictivity (Marshall and Madden, 1959; Kobranova, 1986; Schön, 1996).

In traditional practice, IP data are collected by commercial georesistivity meters while acquiring, for example by means of the Electrical Resistivity Tomography, resistivity data (ERT, Barker, 1989). In this case, the IP information is measured by recording the IP decay curve in the time-domain over one or several time windows following a delay after current switch-off and in this case the measured quantity defines the mediums chargeability η.

The chargeability provides additional independent information, which in many circumstances helps to shed more light on the subsurface. It is used, since its discovery, for metallic minerals exploration; nowadays, the method gained new popularity for solving environmental issues related to the presence of pollutants in the subsurface, both of inorganic and of organic origin (see e.g. the review paper by Atekwana and Atekwana, 2010).

Throughout the seventies of the past century, geophysicists became aware of the fact that IP may affect the observed decay curve after current switch-off of the inducing magnetic field in TEM method. It was reported that the IP effect occurs in the TEM curves due to presence of the double electrical layers (DEL). Usually, this is the electro-osmosis effect. The electrically polarizable bodies/layers affect the decay curves, showing narrow minima, often so strong to give a typical sign reversal. The phenomenon of sign reversal on TEM sounding curves was observed on permafrost areas (Russia and Canada) and was reported first by Sidorov and Yakhin (1979) (see also Walker and Kawasaki, 1988).

* Corresponding author.
E-mail addresses: valeriya.hallbauer@gmail.com (V.Y. Hallbauer-Zadorozhnaya), g.santarato@unife.it (G. Santarato), nsa@unife.it (N. Abu Zeid), samuel.bignardi@unife.it (S. Bignardi).

http://dx.doi.org/10.1016/j.jappgeo.2016.07.014
0926-9851/

During the last 35 years the IP effect on TEM surveys was observed in many areas around the world and in all conditions: in Russia (as an example: Kozhevnikov and Antonov, 2006), in Africa (Hallbauer-Zadorozhnaya and Stettler, 2006), on the permafrost and in the shields, on land and airborne (Smith et al., 2008). Usually for the description of IP effect on TEM sounding the equivalent circuit diagrams of the Cole–Cole model (1941) are used. The presence of IP effect was dealt with by developing specific algorithms being implemented in computer codes to both model it (Ingeman-Nielsen and Baumgartner, 2006; Barsukov and Fainberg, 2001; software TEM RESEARCHER, www.aemr.net) and consequently to remove it (Antonov and Shein, 2008). Usually the decay constant τ of the IP effect observed in the TEM signals is very short, from several microseconds to not more than 1–2 ms (Hallbauer-Zadorozhnaya and Bessonov, 2002).

Recently Zadorozhnaya discovered that both chargeability and resistivity of freshwater saturated samples of different rock types depend on time and intensity of the polarizing direct current (Zadorozhnaya, 2008; Zadorozhnaya and Hauger, 2009; Zadorozhnaya and Maré, 2011). In particular, they observed that chargeability always decreases with increasing current intensity, while resistivity can both increase and decrease. Increasing time of current pulses resulted in an increase of both resistivity and chargeability values. The observed non-linearity of chargeability increase with time is known to be a common occurrence and can be easily understood, however, the remaining non-linear phenomena were quite surprising. That IP could be, under specific conditions, a non-linear phenomenon due to current increase, was a circumstance of which, in early times of the method, scientists were aware of Bleil (1953), although the reasons were not further investigated. Few decades later, one of the authors (G. Santarato in Iliceto et al., 1982) was involved in a paper about laboratory IP measurements on samples of loose sediments (clay, silt and sand), where it was claimed that all the measurements were performed in the range of supplied currents that ensured the linear behavior of the IP response.

A reason for such omission could be the fact that this "anomalous" behavior is observed only in the lab where employed current densities are orders of magnitude greater than those normally available in field measurements, mainly for safety and portability of current sources. In addition, the non-linearity dependence on charging time was observed using longer charging times than those normally used in field surveys.

In the Zadorozhnaya's cited papers, a physical–mathematical model was developed and discussed. The model accounts for the observed non-linear behavior in the tested rock samples. She showed that the non-linearity can be explained by a specific solution of the equations governing the phenomenon of membrane polarization invoking the concept of constrictivity of pores. Results of the fieldwork carried out in a purposely selected study area in northern Italy showed that non-linearity can be observed in the field too, provided a specific setup of field measurements is designed (Hallbauer-Zadorozhnaya et al., 2015).

We assume that the recorded signals are distorted both by electro-osmosis and membrane IP and our task is to assess the contribution of both of them, bearing in mind that our definite task is to provide a reliable geological interpretation of TEM data.

In the following we will consider the mechanisms of both electro-osmosis and membrane IP effects.

1.1. Electro-osmosis effect

The electro-osmosis polarization arises as a result of the transport of the electrolyte through the sediments when a gradient in the electrical field is applied. This will move some of the cations from the diffusion part of the electrical double layer (EDL) d into free solution, relative to the solid medium (Fig. 1). An electric field is thus generated which in its turn produces a gradient of fluid pressure. After the field returns to zero (TEM off-time) that pressure gradient moves the pore fluid in the opposite direction, and this process generates an electro-osmosis potential V_{EO}.

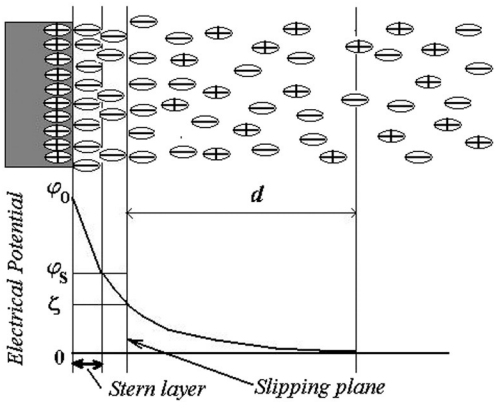

Fig. 1. The sketch of the double electric layer (DEL). d is the thickness of the diffusion part of DEL, φ_0 and φ_s are potentials on inner and outer Helmholtz planes accordingly, ζ is zeta potential.

It is well known that numerous formulas describe the IP-effect: they were collected and analyzed by Diaz (2000). The most widely used IP model is described by the Cole–Cole model (Cole and Cole, 1941, Pelton et al., 1978) given in general form in the frequency-domain as:

$$\rho(\omega) = \rho_0\left\{1-\eta\left[1-\frac{1}{1+(i\omega\tau)^c}\right]\right\}, \tag{1}$$

where ρ_0 is the resistivity at 0 frequency (in $\Omega\cdot$m), η is the chargeability (dimensionless), τ is the decay time (in s) and c is a parameter which takes a steady value, between 0 and 1, and allows describing different spectral shapes (dimensionless). The Cole–Cole model can be written as a function of a complex conductivity as well:

$$\sigma(\omega) = \frac{\sigma_0}{1+\frac{\eta}{1+(i\omega\tau)^c}}, \tag{2}$$

where $\sigma_0 = \frac{1}{\rho_0}$. For interpretation of TEM data usually the Eq. (2) with $c = 1$ is used and in time domain the Eq. (2) becomes, by Fourier transform:

$$\sigma(t) = \frac{\sigma_0}{1+\eta}\left[1-\eta\cdot\exp\left(-\frac{1-\eta}{\tau}t\right)\right], \tag{3}$$

The parameters which characterize the electro-osmosis IP effect are polarizability η and decay constant τ. These parameters are considered below. In porous media due to the presence of DEL, concentration of cations C_k and anions C_a and the transfer numbers n_k and n_a, can be different (subscripts k and a indicate cations and anions, respectively). Transfer numbers define the ratio of electrical current transferred by ions and they differ from those which are observed in free solution. It is also known that the specific electrical conductivity of an electrolyte in the pores of a medium is proportional to the mobility of the ions μ, and to the sum of their concentrations (Fridrikhsberg, 1995):

$$\sigma_\chi = zF\mathrm{M}(C_a - C_k) \text{ and } \sigma_\Delta = zF\mathrm{M}(C_a + C_k), \tag{4}$$

where σ_χ is the conductivity of pores fluid (excess of cations) and σ_Δ is the conductivity of the dense and diffuse layers of DEL (excess of anions), F is the Faraday's constant, and z is the valence of the ions. Plus "+" and minus "−" signs are used here because cations and anions have opposite charges. When the electrical current is turned on, the surplus of ions of one charge prevents the flow of

an electrical current. Hallbauer-Zadorozhnaya and Bessonov (2002) showed that the chargeability η can be written as:

$$\eta = \frac{\sigma_\Delta}{\sigma_\chi}. \tag{5}$$

This means that η is the ratio of electrical conductivity surplus to the electrical conductivity of the pore fluid. According to Eq. (5) the values of polarizability η can be in the range from 0, for sediments with large pore radiuses when the contribution of the EDL is negligible, to 1, in sediments such as some types of clay, where the pore radii are very small and $\sigma_\Delta \approx \sigma_\chi$ (all anions are immobile and represent the dense and diffuse layers whereas all cations are dissolved in a fluid and able to carry electrical current).

Hallbauer-Zadorozhnaya and Bessonov (2002) also showed that the time decay depends on square of pore radius r:

$$\tau = \frac{(1-\eta)r^2}{5.78\nu_k}, \tag{6}$$

where ν_k is the dynamic viscosity of fluid.

Electro-osmosis type of polarization is opposite to the current flow. The mechanism of electro-osmosis effect is described by Helmholtz–Smoluchowski equation (Smoluchowski, 1916):

$$I = \frac{\varepsilon\varepsilon_0\zeta}{4\pi\sigma_f} V_f, \tag{7}$$

where I is a secondary electrical current arising due to water flowing through pore, ε is relative dielectric permittivity (dimensionless), ε_0 is the dielectric constant of vacuum ($1/36\pi 10^9$ F/m), ζ is the zeta potential (in V), $\sigma_f$is total conductivity of fluid filled pore (including double electrical layers), and V_f is velocity of water flowing in the pore (in m/s). After turn-off, the secondary current attenuates in accordance with Eq. (3). Quite obviously, there is a linear dependence between water velocity and electrical current, and it does not depend on duration of current pulses provided by the TEM transmitter.

1.2. Membrane polarization effect

The mechanism of membrane polarization (MP) was proposed by Marshall and Madden (1959). Its main source is the presence of clay particles in pores saturated with water. These particles encumber the free circulation of dissolved ions, as they capture cations by adsorption. However the membrane polarization has a number of features as compared with other types of IP effects, namely:

- the membrane polarization can be simply caused by constrictivity of pores, even in absence of clay particles. It occurs whenever electrical current flows through a channel containing pores with different radii: an excess/loss of ions accumulates at the boundaries;
- it follows that the membrane polarization always occurs together with electro-osmosis polarization;
- the membrane polarization is function of concentration difference at pores ends;
- unlike other types of polarization, MP is directed forward to the applied electrical current (Kobranova, 1986).

Let us briefly describe the basic theory of the membrane IP effect. If a pore space contains many parallel capillaries and a DC current is applied, then the cations moving to the cathode will pass the boundary between narrow capillary II and enter to the volume ΔV_A, at the anode side of large capillary I and move further (Fig. 2).

Masses m_{IIk} and m_{Ik} (in moles) of cations and anions which enter into the volume ΔV_A and leave this volume according to Faraday's law

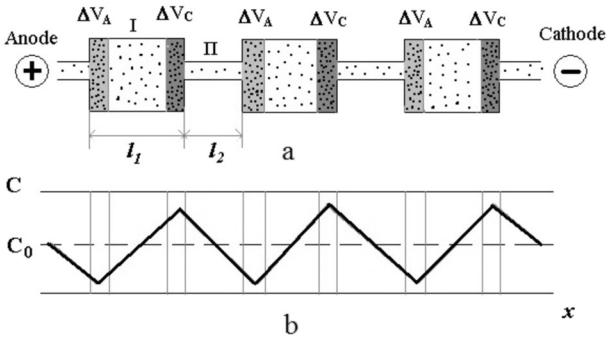

Fig 2. a) Model of capillary: I and II are large and narrow parts of capillary, accordingly, l_1 and l_2 are their lengths, ΔV_C is the small volume of the capillary oriented to the cathode, ΔV_A is the small volume of the capillary oriented to the anode; b) distribution of salinity in the capillary after applying an electrical current, C is the concentration in pore, C_0 is the concentration of electrolyte in free solution: due to presence of DEL they are different (after Fridrikhsberg, 1995).

are equal to (Fridrikhsberg, 1995):

$$m_{IIk} = \frac{q}{Fz_k} n_{IIk} = \frac{It}{Fz_k} n_{IIk}, \quad m_{Ik} = \frac{q}{Fz_k} n_{Ik}, \tag{8}$$

where q is the amount of charge (in Coulomb) that passed through the boundary II–I or I–II, I is the current, F is the Faraday constant, z_k is the valence of cations, n_{IIk} and n_{Ik} are the transfer numbers in narrow and large capillaries (Eq. (8)), respectively.

Obviously, cations in narrow capillaries are more mobile than anions (transfer more electrical charges) because in narrow capillaries some of anions are absorbed by the double electric layers (DEL) and are immobile. In the narrower section, the transfer number of cations can be $n_{IIk} \to 1$ and likewise $n_{IIa} \to 0$. In large capillaries transfer numbers n_{Ik} and n_{Ia} tend to be identical and equal to transfer numbers in free solution ($n_{Ik} = n_{Ia} = 0.5$). In this case the DEL does not play a considerable role on current flow. It was shown (Kobranova, 1986) that if the surface areas of capillaries I and II are different and $n_{IIk} > n_{Ik}$ then:

$$\Delta m_{k\Delta V_{IA}} = m_{Ik} - m_{IIk} = \frac{q}{Fz_k}(n_{IIk} - n_{Ik}) > 0. \tag{9}$$

This means that the salinity of cations in the volume ΔV_{IA} increases (see Fig. 2). The salinity of anions is increased by the same amount (in case of neutrality of solution):

$$\Delta m_{a\Delta V_{IA}} = m_{Ia} - m_{IIa} = \frac{q}{Fz_k}(n_{IIa} - n_{Ia}) > 0. \tag{10}$$

At the boundary II and I, the salinity of cations and anions in volume ΔV_{IC} decreases:

$$\Delta m_{k\Delta V_{IC}} = \frac{q}{Fz_k}(n_{IIk} - n_{Ik}) < 0, \quad \Delta m_{k\Delta V_{IIC}} = \frac{q}{Fz_a}(n_{Ia} - n_{IIa}) < 0. \tag{11}$$

It means that the same amount of cations and anions will accumulate at the contacts of the narrow pore channels and large pores. The difference of concentration occurring due to current flow at the contacts pore/pores channels is the foundation of the phenomenon of membrane polarization. The mathematical problem of ions distribution in a solution filling the pores when a step-like electrical current is applied has been solved by Zadorozhnaya (2008), Zadorozhnaya and Hauger (2009) and Zadorozhnaya and Maré (2011).

The excess of salinity at the boundary between pores depends on time of applied current:

$$u_{\Delta 2k} = \frac{I_k^2 M_k t}{F z_k S_1 S_2 \sigma_k}(n_{2k} - n_{1k}), \quad u_{\Delta 3k} = \frac{I_k^2 M_k t}{F z_k S_1 S_3 \sigma_k}(n_{3k} - n_{1k}),$$
$$u_{\Delta 2a} = \frac{I_a^2 M_a t}{F z_a S_1 S_2 \sigma_a}(n_{1a} - n_{2a}), \quad u_{\Delta 3a} = \frac{I_a^2 M_a t}{F z_a S_1 S_3 \sigma_a}(n_{1a} - n_{3a}), \tag{12}$$

where I is the applied current, t is the time, S_1, S_2 and S_3 are the surface areas of central pore and left and right channels respectively, and where M_k and M_a are average mobilities of cations and anions.

If pulse length is short, then the excess of ions becomes small and the time of leveling (discharging) is also short. Increasing the length of current pulse the membrane effect increases. The direction of ions accumulations in the boundaries is the same as the current flow (Kobranova, 1986), in other words the direction of discharge is also the same as the direction of transient electro-motive force (emf). That is why the resistivity of layers where membrane IP effect occurs can considerably decrease.

2. Materials and methods

2.1. Description of the study site

In 2012, six Transient Electro-Magnetic (TEM) soundings were carried out, in and around the Riolo Terme town (Northern Apennines, Italy), in the framework of the EU financed project "Cities on Power". The aim of the survey was to aid in the reconstruction of the subsurface conceptual model for hydrogeological assessment of a test site, where a pilot low-enthalpy geothermal plant was planned to be installed in a 100 m deep borehole. The local outcropping geological units together with the locations of TEM soundings are shown in Fig. 3. The FAAts Unit is composed mainly of fine sandstone and pelitic argillaceous sediments. The FAA Unit (Blue Clay Unit: Pliocene–Pleistocene) is composed of gray argillaceous mudstones with rare and thin sandstone layers. These units are partially covered by Quaternary deposits belonging principally to the Ravenna Sub-synthem (AES8) whose upper part constitutes the Modena Unit (AES8a, Pleistocene–Holocene). These recent deposits are composed of gravel, silt and sand, whose maximum thickness is around 10 m, and host the phreatic aquifer. Visual inspection of cuttings of the well, drilled in the vicinity of TEM 1 to host the geothermal probe, furnished the following lithological sequence: i) 0–5 m: brown clay with sand; ii) 5–10 m: clayey sand with pebbles (aquifer); iii) 10–20 m: light-gray clay; iv) 20–100 m: deep-gray clay.

2.2. Geophysical survey

As can be seen on Fig. 3, three soundings (1, 2 and 3) were performed over the FAAts Unit, while TEM 4, 5 and 6 were positioned on sediments belonging to the FAA Unit.

The TEM equipment by Zonge Ltd model Zerotem was used for transmitting the pulsed current into a 50 × 50 m square loop and GDP-3224 was used for data acquisition at the center of the loop. To get information down to the requested investigation depth of about 100 m, and the maximum resolution in the shallow subsurface, data acquisition was planned at 32 Hz repeating frequency (the maximum one allowed by the transmitter) and a latest available time gate of 7.8 ms. While acquiring the data, a typical, strong IP distortion was detected in decay curves, at time gates greater than 1 to 2 ms. Because of this result and bearing in mind that the distortion due to IP reduces the investigation depth of TEM method, all decay curves were acquired at the repetition frequencies of 8 Hz (latest time gate at 31.125 ms) and 4 Hz (latest time gate at 62.25 ms), to be sure to reach the planned investigation depth. In all measurements the current pulse amplitude was about 10 A. In Fig. 4 we show the obtained decay curves after current cut-off: data pertaining to soundings 1, 2 and 3, collected above the FAAts Unit show a fair dependence on frequencies of current pulses, as the 32 Hz

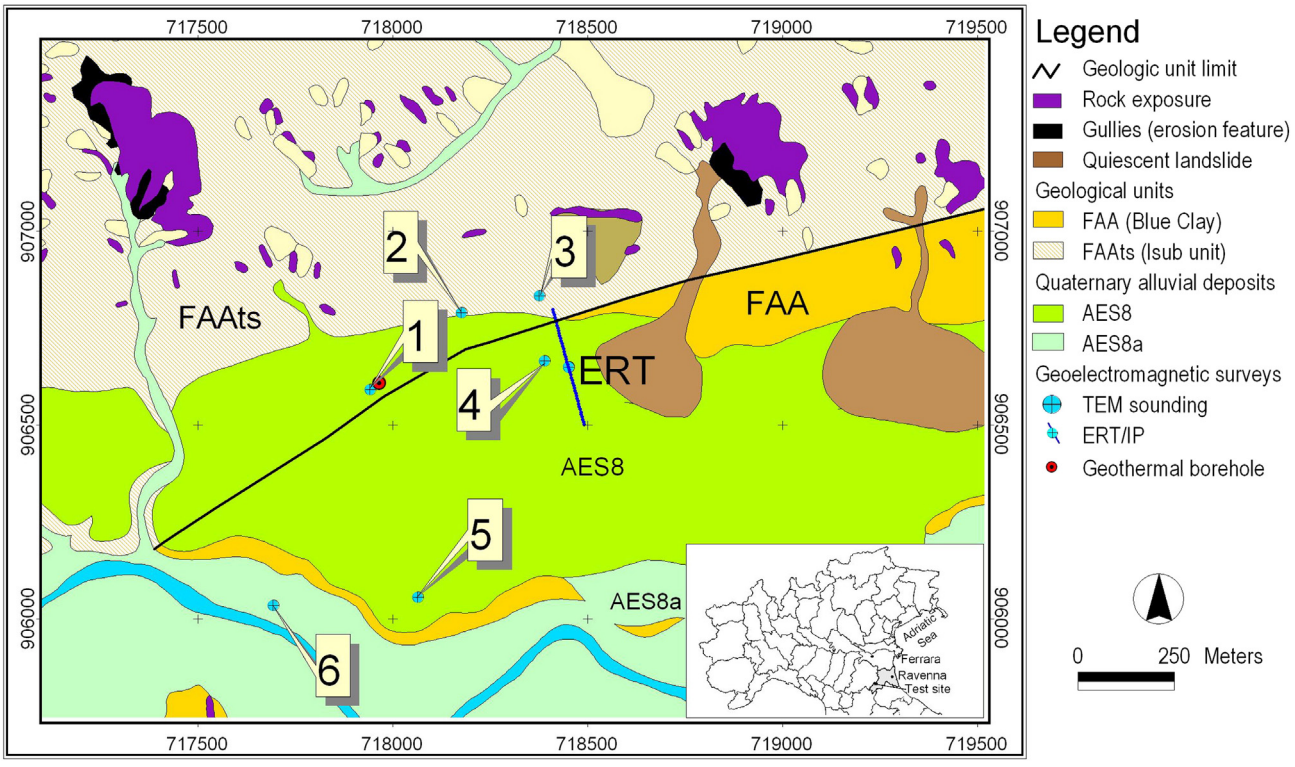

Fig. 3. Location of TEM soundings and ERT profile above the geological map of survey area (redrawn after the Geological Map of Italy 1:50,000, Sheet 239). Coordinates are in m in the European Datum 1950 (ED50, WGS84).

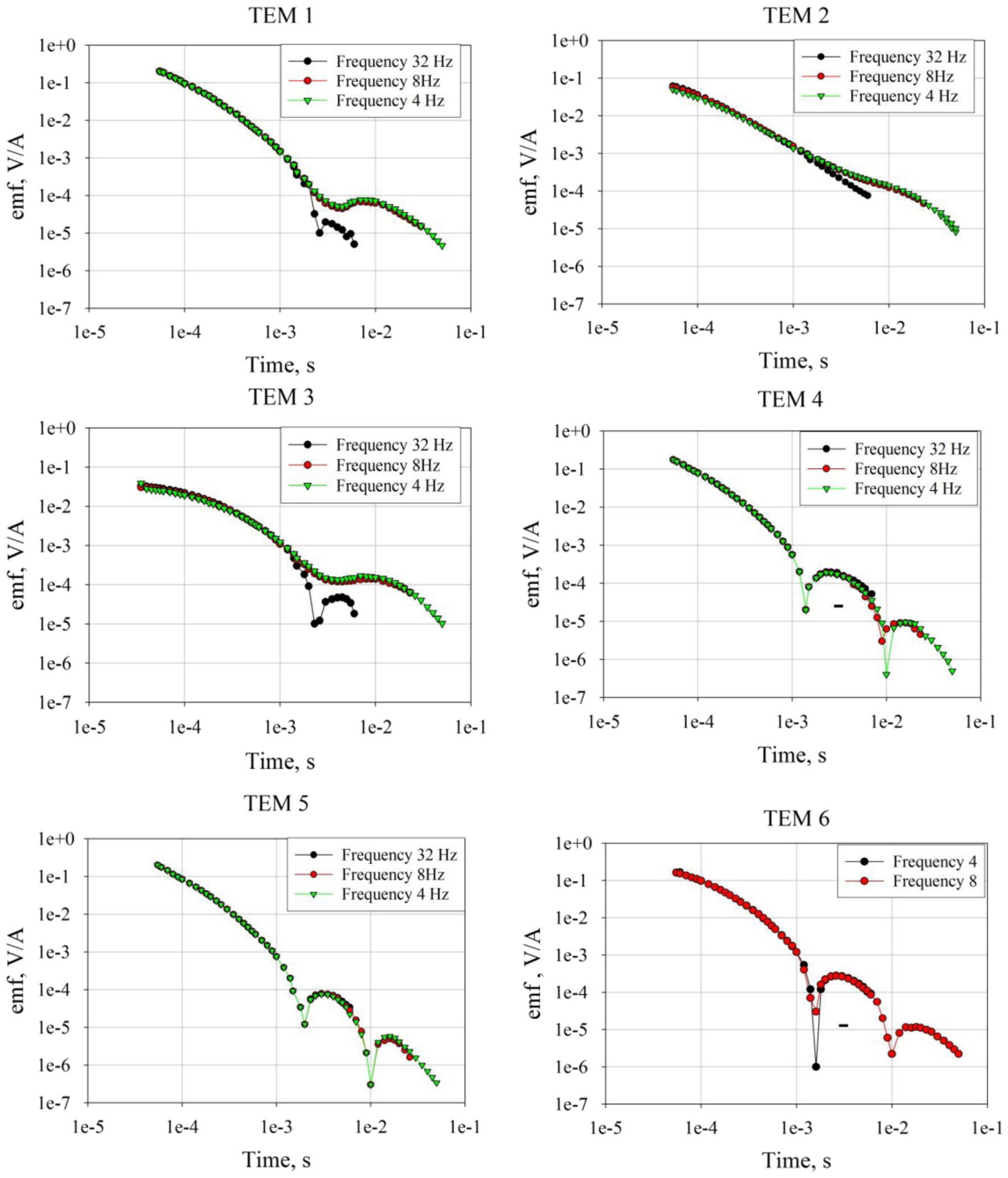

Fig. 4. Decay curves of TEM soundings 1–6.

decay curve strongly differs from 8 Hz and 4 Hz ones, while the decay curves of soundings 4, 5 and 6, collected above the FAA Unit, resulted "classical" for TEM distorted by IP effect, as they do not depend on frequencies of the current pulses.

To cross-check TEM data mainly from the IP point of view, we decided to carry out also a profile of Electrical Resistivity (ERT) and time-domain IP Tomography (indicated as ERT in Fig. 3), where the topographical and urbanization conditions allowed locating it. The profile was laid out above the FAA formation, at the border of FAAts formation, about 50 m East of TEM sounding 4. It was composed of 45 electrodes at 7 m distance between each other, for a whole profile length of 308 m. The georesistivity-meter model SAS4000/ES464 by ABEM Instrument AB (Sweden) was used and the Wenner–Schlumberger array was selected as a good compromise between vertical and lateral resolution. Inversion of apparent resistivity and chargeability data was performed by using the RES2DINV™ commercial software, based on the quasi-Gauss–Newton least-squares minimization algorithm and the minimum smoothness constrained regularization (Loke and Barker, 1996), obtaining a 1.6% RMS error on resistivity model and an absolute error of 0.45 on chargeability model after 5 iterations. The inverted resistivity and chargeability sections are shown in Fig. 5: a substantially 1D subsurface results from the resistivity section, where the upper resistive layer should be identified with Quaternary loose sediments and the substratum with submarine clay formations. The IP section shows a polarizable layer, lying at a depth around 15–20 m below ground level (b.g.l.), characterized by a lateral inhomogeneity. It is worthy to note that, since IP occurs only in presence of saturated media, the IP effect should be associated to the water-saturated part of the upper resistive layer.

Moreover, using a TEM-FAST 48 equipment by AEMR (The Netherlands) and a 25 × 25 square loop, all TEM sites were repeated

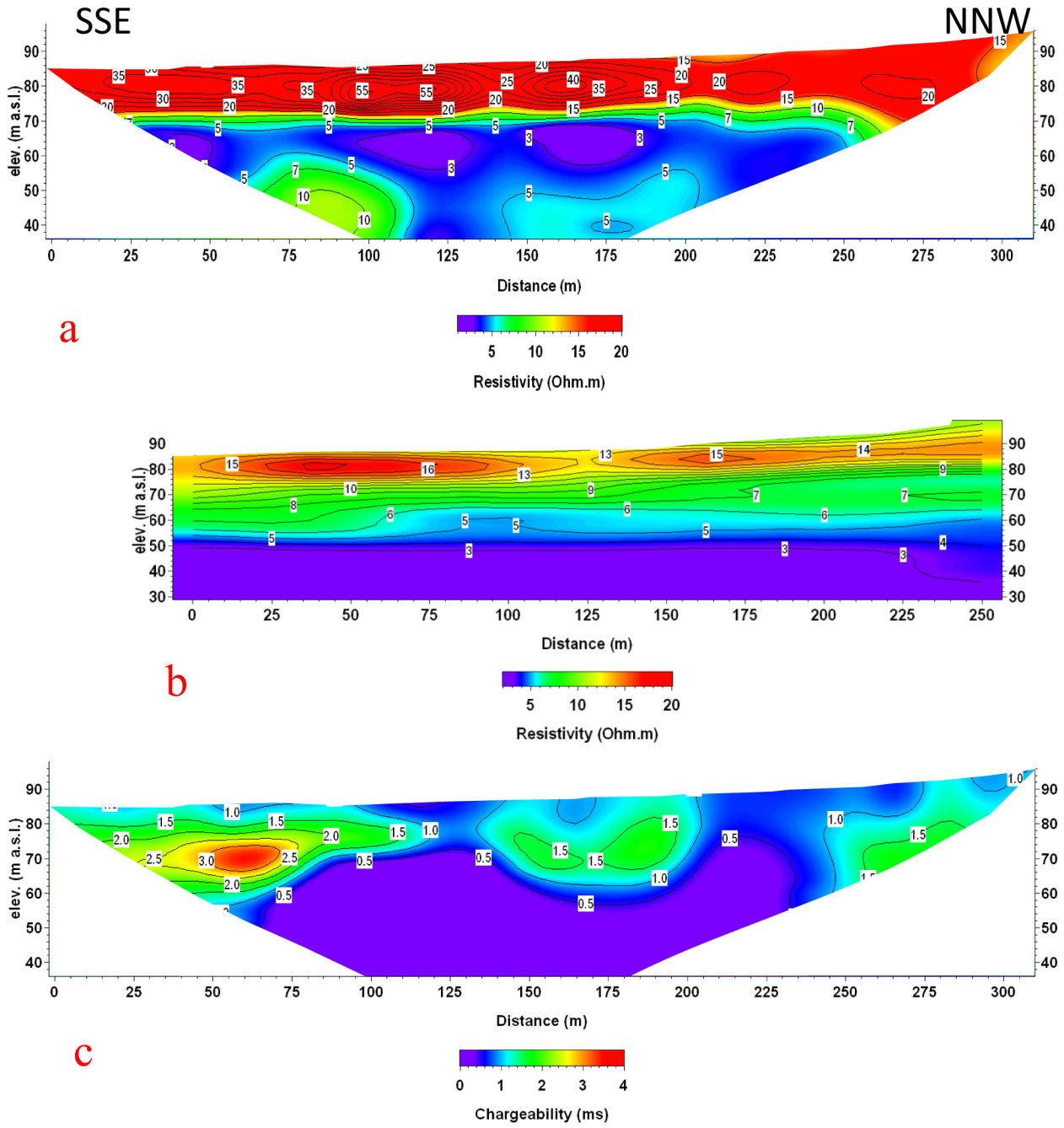

Fig. 5. a) 2D resistivity section along the ERT profile; b) pseudo-2D resistivity section obtained by stacking 11 1D models from TEM data; the TEM profile is aligned with ERT/IP; c) 2D chargeability section along the ERT profile (a.s.l.: above sea level).

and a profile composed of 11 TEM soundings was performed along the ERT profile; a 1 A pulsed current at 50–100 Hz and a maximum time gate of 2 ms were used. With these acquisition parameters, this survey was planned to check whether IP effect could affect these higher frequency data at the latest time gates. However, TEM-FAST decay curves did not show any IP effect. The reason is now clear: we are in the presence of an IP phenomenon which is frequency-dependent and increases with decreasing frequency, i.e. the membrane effect, whose presence is quite evident in TEM soundings 1, 2 and 3. Moreover, this result is conditioned, most probably, by the one order of magnitude smaller current intensity, fed by TEM-FAST. In fact, as shown in Section 1.2, the membrane IP effect depends not only on duration of exciting current pulse, but also on its intensity (see also Hallbauer-Zadorozhnaya et al., 2015). Using the Matlab code IRAF (see Section 3 for more details) to model an 1D subsurface, TEM-FAST data pertaining to the ERT profile were inverted and, stacking the respective best-fitting 1D models, the obtained pseudo-2D resistivity section, shown in Fig. 5b, showed good agreement with the ERT model section.

3. TEM data interpretation

The interpretation of TEM data was carried out using the Matlab code IRAF written by V. Hallbauer-Zadorozhnaya, where the Cole–Cole relaxation Eq. (3) was implemented. The forward model consists of a set of horizontal polarizable layers (Zadorozhnaya and Lepyoshkin, 1998). Results of inversion of TEM 4–6 are given in Table 1, while in Fig. 6 we show the curve of the best fitting model to TEM 4, as an example. The models show a relatively resistive (18 Ω·m) first layer, whose thickness corresponds to the thickness of the Quaternary alluvial sediments, while resistivity of deeper layers gradually decreases with

Table 1
1D petrophysical models of TEM 4, 5 and 6.

TEM	Layer	ρ (Ω·m)	Thickness h (m)	τ (s)	η
4	1	18	13	$2.8 \cdot 10^{-3}$	0.0125
	2	4.3	25	–	–
	3	0.6	∞	–	–
5	1	18	13	$2.7 \cdot 10^{-3}$	0.01
	2	4.3	25	–	–
	3	0.8	∞	–	–
6	1	18	13	$2.9 \cdot 10^{-3}$	0.02
	2	1.7	22	–	–
	3	0.5	35	–	–
	4	0.7	∞	–	–

depth. The resistivity of about 0.5–0.8 Ω·m at depths below 35–40 m is compatible, although quite low, with a clay formation deposited in a submarine environment. Note that the shallowest layer is polarizable and the resistivity of the deepest layer, in all tables presented in this paper, can be considered as the resistivity of the electrical substratum.

These models show a good agreement with the ERT/IP sections shown in Fig. 5.

However the TEM 1–3 decay curves, collected in the northern part of the area, strongly depend on repeat frequencies. We observe a non-linear dependence of recorded signals on length of the pulses at late times, beyond 2 ms. If we try to interpret these soundings using "classical" IP effect model, as for TEM 4–6, we obtain the models listed in Table 2 for, e.g., TEM 3 at 32 and 4 Hz respectively. The parameters obtained at 32 Hz are very similar to the parameters of 1D models of TEM4–6. However, the resistivity of all layers and especially resistivity of clays considerably decreases if data at repetition rates of 8 Hz or 4 Hz are inverted. The resistivity 0.05 Ω·m is much lower than that of sea water and definitely cannot be related to any kind of rocks, although saturated by sea water. Moreover, the polarizability property migrates from the upper electrical layer, saturated with fresh water, to deepest ones, certainly saturated by salt water: it is well known that any kind of polarization, excluding the electrode polarization, is inhibited by the high concentration of dissolved ions, proper of salt water. However, as mentioned above, soundings TEM 1–3 and TEM 4–6 soundings are located above slightly different lithologies: soundings 1–3 are positioned over the FAAts Unit, which is composed, mainly of fine sandstone and

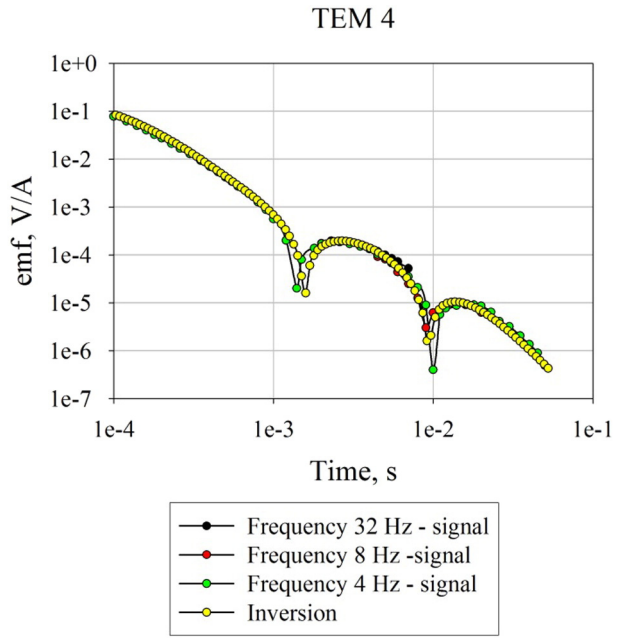

Fig. 6. Data and best-fitting 1D model of TEM 4.

Table 2
1D petrophysical model parameters of TEM 3 using the Cole–Cole equation.

32 Hz repetition rate					4 Hz repetition rate				
Layer	ρ (Ω·m)	h (m)	τ (s)	η	Layer	ρ (Ω·m)	h (m)	τ (s)	η
1	90	15	–	–	1	30	30	–	–
2	12	25	–	–	2	8	45	–	–
3	2.3	19	–	–	3	0.92	45	$3 \cdot 10^{-3}$	0.25
4	0.5	20	$3.5 \cdot 10^{-3}$	0.25	4	0.05	45	$3.5 \cdot 10^{-3}$	0.99
5	0.5	25	$3 \cdot 10^{-3}$	0.25	5	0.05	∞	$3 \cdot 10^{-3}$	0.99
6	0.6	∞	$3 \cdot 10^{-3}$	0.25					

pelitic argillaceous sediments, while soundings 4–6 are located on AES8, AES8a formations, which lie over the FAA Blue Clay lithological Unit, composed mainly of gray argillaceous mudstones with rare thin sandstone layers. In simpler words, there is a presence of arenaceous, coarser sediments in the sequence pertaining to FAAts Unit.

It was already reported that specific porous lithologies, in particular sandstone, can exhibit a non-linear behavior: their resistivities and chargeabilities depend on intensity and duration of the supplied electrical current. This effect was studied and characterized both on laboratory samples (Zadorozhnaya, 2008; Zadorozhnaya and Hauger, 2009; Zadorozhnaya and Maré, 2011) and in the field (Hallbauer-Zadorozhnaya et al., 2015). Thus the non-linear effect vs. repetition frequency of supplied current, observed in TEM soundings 1–3, could be explained if we accept that a type of IP effect occurs, which depends on different length of current pulses, i.e., as shown above, by the membrane IP effect.

3.1. Interpretation of TEM data depending on current pulse length

That membrane polarization affects non-linearly TEM data, to our knowledge, has never been reported in the scientific literature. It is a new phenomenon (at least, to our knowledge). We assume that it is a membrane IP superimposed to the induction process and to electro-osmosis IP effect. As indicated above, the membrane IP is only one type of polarization depending on time of current feeding, which is directed concordant to applied electrical current, i.e. it has the same positive sign.

The problem for diffusion exchange with host media for time-off is to be described by the inhomogeneous diffusion equation with specific boundary and initial conditions:

$$\frac{\partial u}{\partial t} = a^2 \frac{\partial^2 u}{\partial x^2} + f(x,t), \tag{13}$$

where $f(x,t)$ is a function of the diffusion sources. It is assumed that the function $f(x,t)$ has a piecewise-continuous derivative of the first degree by x. Let us note that the initial conditions must be found at time-on case, from the above described problem of the distribution of electrolyte concentration. It was shown that it can be solved according to the Fourier method using the partial solutions (Koshlyakov et al., 1970):

$$u_n(x,t) = X_n(x) \cdot T_n(t), \tag{14}$$

where $X(x)$ is a partial solution depending on x (distance along the pore) and $T(t)$ depends on time t. The full solution of Eq. (13) is:

$$u(x,t) = \sum_{n=1}^{\infty} X_n T_n, \tag{15}$$

where

$$T_n = \alpha_n \exp\left[\left(-\frac{\mu_n a}{l}\right)^2 t\right], \tag{16}$$

where α_n are the arbitrary constants, n is the number member of series, l is the pore length, and μ are parameters depending on coefficients of ion exchange. The solution of the problem of ions exchange caused by constrictivity of pores, with specific boundary conditions, is described in detail by Zadorozhnaya and Maré (2011).

The Eq. (15) is the solution for membrane polarization at time-off and consists of numerous exponents. For preliminary interpretation we assume that the membrane IP effect could be modeled using Cole–Cole model with opposite sign. We added a new function which is a mirror image of Cole–Cole model taking note also of the amplitude of membrane effect.

$$p_{ME} = \alpha_2 \frac{\eta_2}{\tau_2} \exp\left(-\frac{1-\eta_2}{\tau_2} t\right), \tag{17}$$

where η_2, τ_2 and α_2 are chargeability, decay constant and coefficient of attenuation respectively. The IRAF code was modified adding the Eq. (17). The results of the inversion are shown in Table 3, while in Fig. 7 we show the curve of the best fitting model of TEM 3, as an example.

As is shown in Table 3, models of soundings 1, 2 and 3 resume resistivity values satisfactorily compatible with those estimated from the soundings in the southern area, with the ERT resistivity profile and definitely with the known geology. In particular, inversion of TEM 1, located very near to the geothermal well, indicates that the upper layer, 11 m thick, essentially coincides with the shallowest formation, 10 m thick, characterized by a clayey sand texture. Moreover, the upper layer comes to be polarizable, in agreement with all other models of TEM soundings 4–6 and IP 2D section, while polarizability in deep layers vanishes. We would like to note the decay constants τ_2's related to membrane effect, are much larger than τ_1's, which are related to electro-osmosis effect. As a final remark, we observe that, invoking the above described theory about non-linear response of TEM data vs. repeat frequency, we obtained resistivities at depth for TEM soundings 1–3 which are in better agreement with the ERT 2D model of Fig. 5a, than those of TEM soundings 4–6: in fact, from a petrophysical point of view, resistivities in the range 1.1 to 1.8 Ω·m are much more proper for a clayey formation, deposited in a submarine environment (see, e.g., Abu-Zeid and Santarato, 2004). We feel that a small non-linear effect, although not detectable on the collected data because of the discrete sequence of time windows, is present also in the decay curves 4–6. In fact, the inverted resistivities of deeper layers (see Table 1) are, as already observed, quite low to be fully compatible with the electrical properties of the local geology: then it is plausible that these decay curves are distorted too, although in a much lower amount, in the same sense of TEM 1–3 curves. This consideration is supported by the slight existing differences between the two FAA and FAAts geological Units.

Table 3
1D petrophysical models of TEM1, 2 and 3:

Sounding	Layer no.	ρ (Ω·m)	Thickness (m)	Electro-osmosis effect parameters		Membrane polarization parameters		
				τ_1 (s)	η_1	τ_2 (s)	η_2	α_2
1	1	23	11	0.033	$3.7 \cdot 10^{-3}$	0.32	$6.8 \cdot 10^{-3}$	0.12
	2	2.8	26	–	–	–	–	–
	3	1.5	25	–	–	–	–	–
	4	1.8	∞	–	–	–	–	–
2	1	30	28	0.014	$1.2 \cdot 10^{-2}$	0.35	$2.0 \cdot 10^{-2}$	0.17
	2	1.5	25	–	–	–	–	–
	3	1.1	25	–	–	–	–	–
	4	2.0	∞	–	–	–	–	–
3	1	50	28	0.032	$4.0 \cdot 10^{-3}$	0.5	$2.0 \cdot 10^{-2}$	0.17
	2	1.5	25	–	–	–	–	–
	3	1.1	25	–	–	–	–	–
	4	2.0	∞	–	–	–	–	–

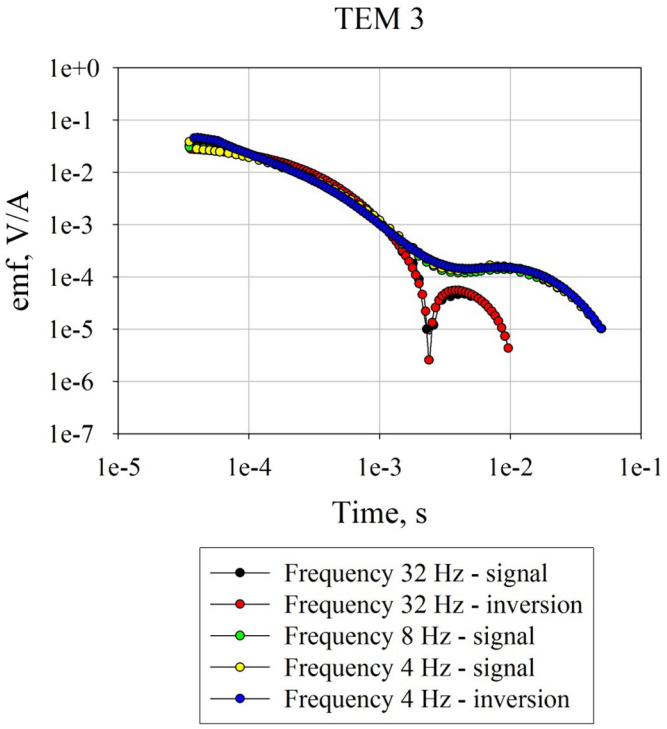

Fig. 7. Data and best-fitting 1D model of TEM 3.

4. Conclusions

A new phenomenon has been observed: TEM decay curves affected by IP show a dependence on current pulse length. Obviously Cole–Cole model cannot be used because, besides not being directly related to physical parameters of rocks, it fits a linear response of a polarizable medium, i.e. not depending on current pulse intensity or length. The membrane polarization effect has been shown to be non-linear vs. both intensity and duration of the supplied electrical current. Therefore this phenomenon was investigated and an algorithm for mathematical modeling of this non-linear observed behavior of the TEM data was developed. The obtained results furnished consistent subsurface physical 1D models.

Acknowledgments

This work was supported by the Natural Research Foundation of South Africa (Grant UID74330) and by the Italian Ministry of Foreign Affairs (Grant ZA14MO02). Province of Ravenna, partner of the project Cities on Power, of EU Transnational Program "Central Europe", 2007–2013, GA Nr. 3CE302P3, is acknowledged for the financial support of the geophysical survey at the Riolo Terme site and for permission to publish the data.

References

Abu-Zeid, N., Santarato, G., 2004. On the correspondence between resistivity and texture of loose sediments, saturated with salt water. Near Surf. Geophys. 2, 144–149.
Antonov, E.Y., Shein, A.N., 2008. Improving inversion quality for IP-affected TDEM data. Russ. Geol. Geophys. 49, 790–802.
Atekwana, E.A., Atekwana, E.A., 2010. Geophysical signatures of microbial activity at hydrocarbon contaminated sites: a review. Surv. Geophys. 31, 247–283.
Barker, R.D., 1989. Depth of investigation of collinear symmetrical four-electrode arrays. Geophysics 54, 1031–1037.
Barsukov, P.O., Fainberg, E.B., 2001. Superparamagnetic effect over gold and nickel deposits. Eur. J. Environ. Eng. Soc. 6, 61–72.

Bhattacharyya, B.K., 1964. Electromagnetic fields of a small loop antenna on the surface of a polarizable medium. Geophysics 29, 814–831.
Bleil, D.F., 1953. Induced polarization: a method of geophysical prospecting. Geophysics 18, 636–661.
Cities on Power (2011-2014). European Territorial Cooperation Objective, CENTRAL EUROPE Programme, GA Nr. 3CE302P3, report 3.4.5. www.citiesonpower.eu.
Cole, K.S., Cole, R.H., 1941. Dispersion and absorption in dielectrics — I alternating current characteristics. J. Chem. Phys. 9, 341–352.
Diaz, A.C., 2000. Developments in a model to describe low-frequency electrical polarization of rocks. Geophysics 65, 437–451.
Fridrikhsberg, D.A., 1995. Course of Colloid Chemistry, Khimiya, SPb. (400 pp. (in Russian)).
Hallbauer-Zadorozhnaya, V.Y., Bessonov, A.D., 2002. The IP effect in TEM soundings applied to a study of ground water pollution by hydrocarbon compounds in Saratov, Russia. Eur. J. Environ. Eng. Geophys. 7, 239–264.
Hallbauer-Zadorozhnaya, V.Y., Stettler, E.H., 2006. The detection of hydrocarbon contaminated of groundwater by using the IP effect in TDEM soundings. S. Afr. J. Geol. 109, 529–540.
Hallbauer-Zadorozhnaya, V.Y., Santarato, G., Abu Zeid, N., 2015. Non-linear behaviour of electrical parameters in porous, water-saturated rocks: a model to predict pore size distribution. Geophys. J. Int. 202, 883–897.
Iliceto, V., Santarato, G., Veronese, S., 1982. An approach to the identification of fine sediments by induced polarization laboratory measurements. Geophys. Prospect. 30, 331–347.
Ingeman-Nielsen, T., Baumgartner, F., 2006. CR1Dmod: a Matlab program to model 1D complex resistivity effects in electrical and electromagnetic surveys. Comput. Geosci. 32, 1411–1419.
Kobranova, V.N., 1986. Petrophysics. Nedra, Moscow (392 pp. (in Russian)).
Koshlyakov, N.S., Gliner, E.B., Smirnov, M.M., 1970. Partial Differentiation of Equations in Mathematical Physics. Vysshayashkola, Moscow (710 pp. (in Russian)).
Kozhevnikov, N.O., Antonov, E.Y., 2006. Fast-decaying IP in frozen unconsolidated rocks and potentialities for its use for permafrost-related TEM studies. Geophys. Prospect. 64, 383–397.
Loke, M.H., Barker, R.D., 1996. Rapid least-squares inversion of apparent resistivity pseudosections using a quasi-Newton method. Geophys. Prospect. 44, 131–152.
Marshall, D.J., Madden, T.R., 1959. Induced polarization, a study of its causes. Geophysics 24, 790–816.
Pelton, W.H., Ward, S.H., Hallof, P.G., Sill, W.R., Nelson, P.H., 1978. Mineral discrimination and removal inductive coupling with multifrequency IP. Geophysics 43, 588–609.
RES2DINV™, 2012. Two-dimensional inversion of apparent resistivity and Induced Polarization data. Version 3.57. Commercial software. http://www.geotomosoft.com.
Schön, J.H., 1996. Physical properties of rocks: fundamentals and principles of petrophysics. In: Helbig, K., Treitel, S. (Eds.), Handbook of Geophysical Exploration — Seismic Exploration vol. 18. Elsevier Scientific Ltd. (222 pp.).
Sidorov, V.A., Yakhin, A.M., 1979. Induced polarization occurred due to induction excitation. Izv. Phys. Solid Earth 15, 46–52.
Smith, R.S., Cheng, L.Z., Chouteau, M., 2008. Using reversed polarity airborne transient electromagnetic data to map tailings around mine sites. Lead. Edge 27, 1470–1478.
Smoluchowski, M., 1916. DreiVorträgeüber Diffusion, BrownscheMolekularbewegung und Koagulation von Kolloidteilchen. Physikzeitschrift (in German) 17, 557–571.
Walker, G.G., Kawasaki, K., 1988. Observation of double sign reversals in transient electromagnetic central induction soundings. Geoexploration 25, 245–254.
Zadorozhnaya, V.Y., 2008. Resistivity measured by direct and alternating current: why are they different? Adv. Geophys. 19, 45–59.
Zadorozhnaya, V.Y., Hauger, M.H., 2009. Mathematical modelling of membrane polarization occurring in the rocks when an electrical field is applied. Phys. Solid Earth 45, 1038–1054.
Zadorozhnaya, V.Y., Lepyoshkin, V.P., 1998. Induced polarization effect on the inductive sounding of multilayered sections. Izv. Phys. Solid Earth 34, 314–320.
Zadorozhnaya, V.Y., Maré, L.P., 2011. New model of polarization of rocks: theory and application. Acta Geophys. 59, 262–295.